

NUMERICAL STUDY OF DISTRIBUTED HYDRODYNAMIC FORCES ON CIRCULAR HEAVE PLATES BY LARGE EDDY SIMULATIONS

Shi-Ning Zhang¹ and Takeshi Ishihara²

¹Economic & Technology Research Institute, Global Energy Interconnection Development and Cooperation Organization, 100031 Beijing, China

²Department of Civil Engineering, The University of Tokyo, 7-3-1, Hongo, Bunkyo-ku, Tokyo, Japan

Distributed hydrodynamic forces on circular heave plates are investigated by Large Eddy Simulation (LES) with volume of fluid (VOF) method. The predicted added mass and drag coefficients for a whole heave plate is firstly validated by water tank tests. The distributions of hydrodynamic loads on the circular heave plates are then investigated. It is found that maximum dynamic pressure occurs at plate center and decreases monotonically towards the outer regions. Finally, formulas of the distributed added mass and drag coefficients in the radial direction are proposed based on the numerical simulations, and effects of aspect ratio and diameter ratio on the distributed added mass and drag coefficients are investigated.

Keywords: Distributed hydrodynamic load, Large Eddy Simulation, Formulas of the distributed added mass and drag coefficients

INTRODUCTION

In the semi-submersible and advanced spar FOWTs, heave plates are commonly used to reduce heave motions and to shift heave resonance periods out of the first-order wave energy range [1]. The hydrodynamic characteristics of the heave plates are key factors during designs of platform that support the floating offshore wind turbine (FOWT). In order to accurately predict dynamic motion of the heave plates in oscillating flows, the distributed hydrodynamic load on the plate is necessary. In addition, accurate load distribution is needed for structural design. The distributed hydrodynamic load are, therefore, needed to be studied.

Computational Fluid Dynamics (CFD) is an alternative way to investigate the hydrodynamic load distribution. Holmes et al. [2] studied the hydrodynamic coefficients of a square heave plate via a finite element method with LES turbulent model. Detailed load distribution on the plate were obtained, but the distributed C_a and C_d was not evaluated. As concluded from previous studies [1, 3, 4, 5], the C_a and C_d are functions of aspect ratio, diameter ratio and KC number. However, the effect of these parameters on distributed C_a and C_d has not been studied yet.

Formulas are cost-effective compared with water tank tests and numerical simulations and are beneficial for optimized design of heave plates. The C_a and C_d for a whole heave plate are studied in the references [5, 6, 7, 8, 9]. However, formulas of the distributed C_a and C_d have not been proposed yet.

NUMERICAL MODEL

Schematic of the heave plate model is shown in Fig. 1. A circular column is attached on the top of the circular heave plate. In order to investigate distributed

hydrodynamic force on the plate in the radial direction, the heave plate is divided into nine annular planes as shown in Fig. 1 (b). The diameter of P1 is 66.8 mm, and space between each adjacent plane is 16.7 mm. Structural grid is generated in the computation domain, and the grid is refined at the locations where substantial flow separation is expected as shown in Fig.2.

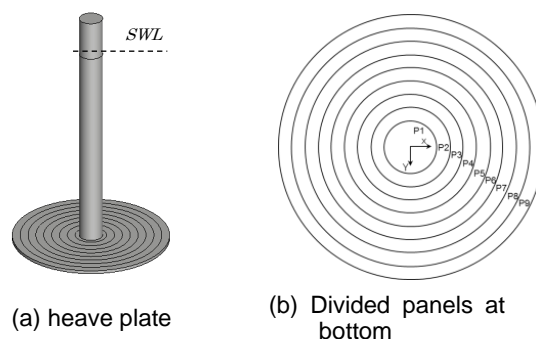


Fig. 1. Schematic of a heave plate and the definition of divided panels.

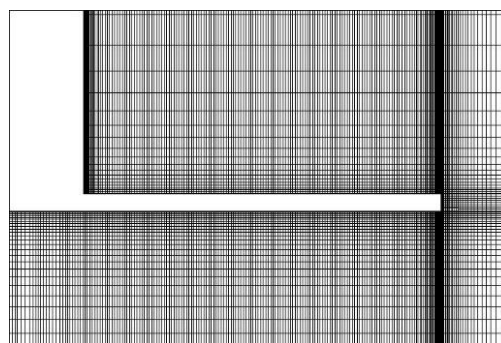


Fig. 2. Grid refinement around edges of heave plate.

In the numerical simulation, the model is vertically oscillated in the sinusoidal form, i.e.,

$$z(t) = a \sin(\omega t) \quad (1)$$

where $z(t)$ is the displacement in the vertical direction from the still water level (SWL), a is the oscillating amplitude, ω is the oscillating frequency ($= 2\pi/T$) and T is the oscillating period.

As introduced in reference [10], Fourier averages of C_a and C_d are obtained as follows:

$$C_a = \frac{\int_0^T F_H(t) \sin(\omega t) dt}{1/3\rho_w D_{Hp}^3 a \omega^2 \int_0^T \sin^2(\omega t) dt} = \frac{3}{\pi \omega a \rho_w D_{Hp}^3} \int_0^T F_H(t) \sin(\omega t) dt \quad (2)$$

$$C_d = -\frac{\int_0^T F_H(t) \cos(\omega t) dt}{1/2\rho_w A(\omega a)^2 \int_0^T |\cos(\omega t)| (\cos(\omega t)) \cos^2(\omega t) dt} = -\frac{3}{4\rho_w A \omega a^2} \int_0^T F_H(t) \cos(\omega t) dt \quad (3)$$

where $F_H(t)$ is the predicted hydrodynamic force acting on the whole heave plate.

RESULTS AND DISCUSSIONS

The time series of the predicted hydrodynamic force is presented in a non-dimensional form as follows:

$$C_F(t^*) = \frac{F_H(t)}{1/2\rho_w S_d(\omega a)^2}; t^* = \frac{t}{T} \quad (4)$$

where $S_d = \pi D_{Hp}^2/4$ is the characteristic area of the heave plate and t^* is the non-dimensional time.

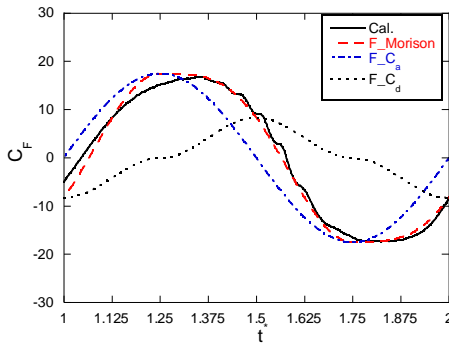
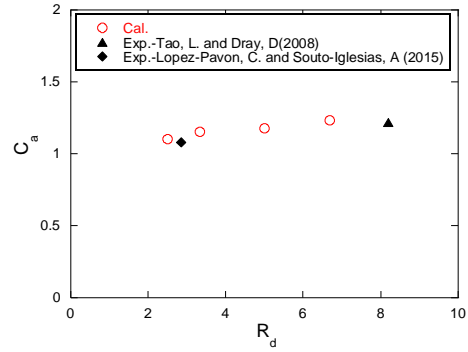
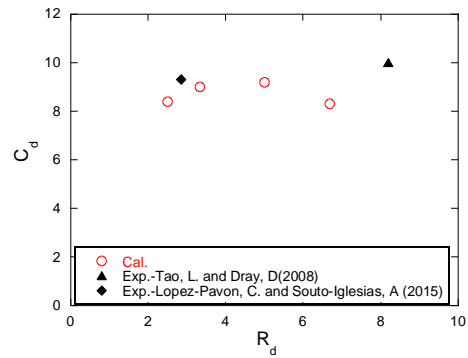


Fig. 3. Time series of non-dimensional hydrodynamic force acting on the whole heave plate.

The time series of non-dimensional hydrodynamic force for one typical case is illustrated in Fig.3. The predicted hydrodynamic force associated with C_a and C_d in the Morison's equation is also plotted in the figure. The hydrodynamic force predicted by Morison's equation matches well with the numerical results in terms of both amplitude and phase.

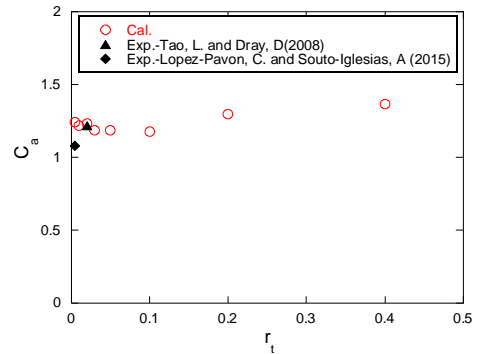


(a) Added mass coefficient

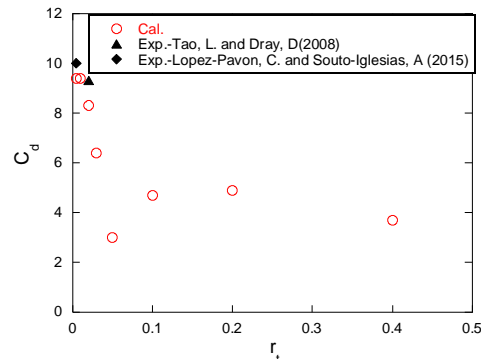


(b) Drag coefficient

Fig. 4. Variation of the added mass and drag coefficients with the diameter ratios.



(a) Added mass coefficient



(b) Drag coefficient

Fig. 5. Variation of the added mass and drag coefficients with the aspect ratios.

Fig. 4 shows the variation of the predicted C_a and C_d and those by the previous studies with diameter ratios. In the experiment by Tao and Dray [26], diameter of the heave plate is 400mm, thickness is 8mm, the diameter of column is measured as 48.8 from their experimental figure. In the experiment by Lopez-Pavon. and Souto-Iglesias [1], diameter of the heave plate is 1000mm, thickness is 5mm, the diameter of column is 350mm. As shown in Fig. 4 (a), C_a slightly increases as the diameter ratio increases. This is because the wet surface at top of heave plate is larger when the diameter of attached column is reduced. The predicted C_a shows good agreement with the measurement. By contrast, C_d shown in Fig. 4 (b) does not increase monotonically with the increase in the diameter ratio because the viscous damping is mainly contributed by the vortex shedding at the outer edges of the heave plate. Increasing the wet surface at top of heave plate has negligible effect on the vortex shedding outside of the center region.

Fig. 5 shows variation of the predicted C_a and C_d with aspect ratios. It can be appreciated from Fig. 5(a) that C_a is independent of the aspect ratio. The change of the thickness has no influence on the characteristic area of upper and lower surfaces of the heave plate, and has no remarkable impact on dynamic pressure distribution. In contrast, C_d is strongly dependent on the aspect ratio as shown in Fig. 5 (b). It is found that C_d decreases as the aspect ratio increases. Variations of the plate thickness generate distinct vortex shedding patterns, which have been reported in the references [3,4,6].

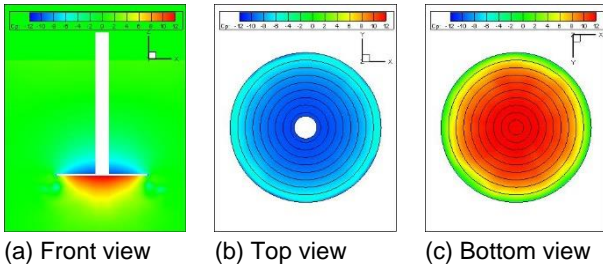


Fig. 6. Distribution of dynamic pressure on the x-z, upper and lower surface of plate at $t=1/4T$.

A pair of positive and negative dynamic pressure is found on the upper and lower surface at time $1/4T$ as shown Fig. 6. At this moment, the dynamic pressure on the upper or lower surfaces gradually decreases from its center to the outer panels, which directly leads to the gradual decrease in the hydrodynamic force.

PROPOSED FORMULAS OF RADIALLY DISTRIBUTED HYDRODYNAMIC COEFFICIENTS

The distributed C_a is assumed to follow an exponential function of Ae^{-Br} . The decay factor B is identified according to the numerically predicted distributed C_a and the coefficient A is evaluated by ensuring the integrated C_a equals to the total value given by the formula proposed by Zhang and Ishihara [6]. formula of the radially distributed C_a is expressed as follows:

$$C_a = \begin{cases} 7.23(1 + 0.2KC)^3 e^{-2.9r}, & r > R_d \\ 0.5[7.23(1 + 0.2KC)^3 e^{-2.9r}], & r \leq R_d \end{cases} \quad (5)$$

where r is the normalized radial distance, KC refers to KC number, and $R_d = D_{HP}/D_c$ represents the diameter ratio, D_{HP} is the diameter of heave plate.

the formula of radially distributed C_d is expressed as follows

$$C_d = \begin{cases} \max(1.7r_t e^{-\frac{1}{3.7}(KC)^{-\frac{1}{2.5}} - 5.08 + 13.9r - 33.4r^2} + 31.3r^3, r > R_d \\ 0.5[\max(1.7r_t e^{-\frac{1}{3.7}(KC)^{-\frac{1}{2.5}} - 5.08 + 13.9r - 33.4r^2} + 31.3r^3), r \leq R_d \end{cases} \quad (6)$$

where $r_t = t_{HP}/D_{HP}$ is the aspect ratio, t_{HP} is the heave plate thickness.

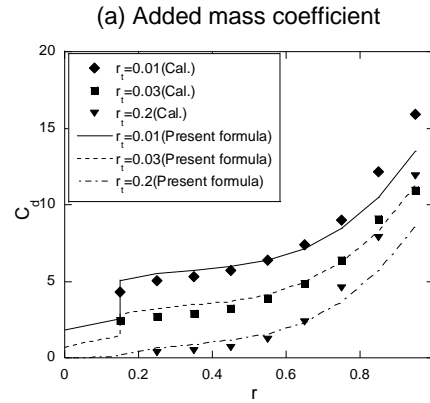
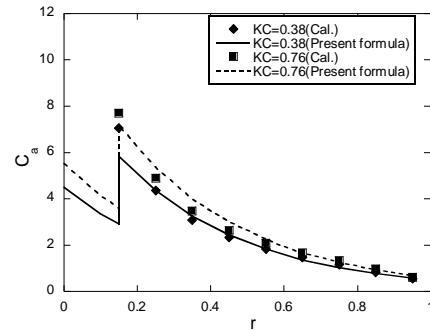
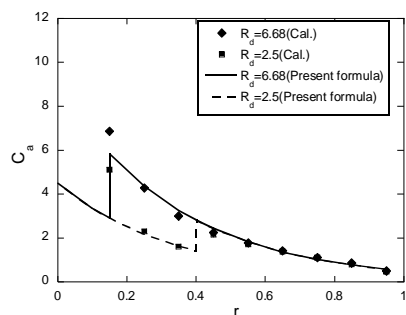


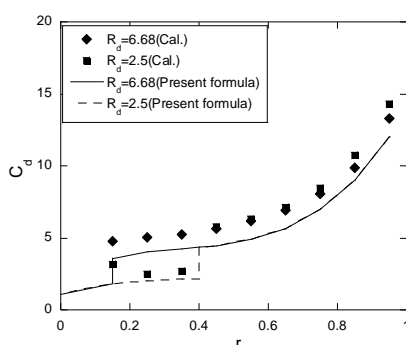
Fig.7. Comparison between the predicted hydrodynamic coefficients and the numerical results for different KC numbers and aspect ratios with $R_d=6.68$.

The distribution of C_a predicted by proposed formula matches well with the numerical results for the different KC numbers as shown in Fig.7(a). From Fig.7(b), the shape of C_d predicted by proposed formula shows good agreement with the numerical results for the different aspect ratios especially in the region near the plate center, while the proposed formula underestimates the C_d near the edge of the plate. The change of vortex shedding pattern around the edge of plate makes the prediction of C_d far more complex which is expected to be improved in future study by introducing one specific parameter to

consider the vortex shedding pattern change. The difference near the column is due to the three-dimensionality of the flow in this region.



(a) Added mass coefficient



(b) Drag coefficient

Fig. 8. Comparison between the predicted predicted hydrodynamic coefficients and the numerical results for different diameter ratios with $r_t=0.02$ and $KC=0.38$.

Fig.8 presents comparison between the predicted hydrodynamic coefficients and the numerical results for different diameter ratios with $r_t=0.02$. The proposed piecewise function of C_a matches well with the numerical results. The distributed C_d by the proposed formula is slightly underestimated due to the underestimation of total C_d for this aspect ratio of 0.02.

CONCLUSIONS

A numerical study of distributed hydrodynamic forces on circular heave plates is performed by large eddy simulation (LES) with volume of fluid (VOF) method. Following conclusions are obtained:

1. The distributed hydrodynamic force on the heave plate is investigated by the flow visualization. The hydrodynamic load decreases with the distance from the center of heave plate and the difference in the time series of the hydrodynamic forces on the inner and the most outer panels is caused by the vortex shedding around the outer edge of heave plate.

2. The added mass coefficient decreases with the distance from the plate center to the outer edge, while the drag coefficient increases from the center to the outer

edge due to the vortex shedding at the outer edge of the plate. In addition, the effect of aspect and diameters ratio on the distributed hydrodynamic coefficients shows the same tendency as the whole hydrodynamic coefficient of the heave plate.

3. Formulas of the distributed C_a and C_d in the radial direction are proposed and validated by the present numerical simulations. The predicted distributions of C_a and C_d show favorable agreement with the numerical simulations for different diameter and aspect ratios.

Acknowledgement

This research is carried out as a part of the Fukushima floating offshore wind farm demonstration project funded by the Ministry of Economy, Trade and Industry. The authors wish to express their deepest gratitude to the concerned parties for their assistance during this study.

References

- [1] Lopez-Pavon, C. and Souto-Iglesias, A. Hydrodynamic coefficients and pressure loads on heave plates for semi-submersible floating offshore wind turbines: A comparative analysis using large scale models. *Renewable Energy*, 2015. 81: p. 864-881.
- [2] Holmes, S., Bhat, S., Beynet, P., Sablok, A., and Prislun, I. Heave plate design with computational fluid dynamics. *Journal of Offshore Mechanics and Arctic Engineering*, 2001. 123(1): p. 22-28.
- [3] Tao, L. and Thiagarajan, K. Low KC flow regimes of oscillating sharp edges. II. Hydrodynamic forces. *Applied ocean research*, 2003. 25(2): p. 53-62.
- [4] Tao, L. and Thiagarajan, K. Low KC flow regimes of oscillating sharp edges I. Vortex shedding observation. *Applied ocean research*, 2003. 25(1): p. 21-35.
- [5] Tao, L. and Cai, S. Heave motion suppression of a Spar with a heave plate. *Ocean Engineering*, 2004. 31(5): p. 669-692.
- [6] Zhang, S. and Ishihara, T. Numerical study of hydrodynamic coefficients of multiple hulls by large eddy simulations with volume of fluid method. *Ocean Engineering*, 2018. 163: p.583-598,
- [7] Tao, L., Molin, B., Scolan, Y.-M., and Thiagarajan, K. Spacing effects on hydrodynamics of heave plates on offshore structures. *Journal of Fluids and Structures*, 2007. 23(8): p. 1119-1136.
- [8] Graham, J. The forces on sharp-edged cylinders in oscillatory flow at low Keulegan–Carpenter numbers. *Journal of Fluid Mechanics*, 1980. 97(02): p. 331-346.
- [9] Philip, N.T., Nallayarasu, S., and Bhattacharyya, S. Experimental investigation and CFD simulation of heave damping effects due to circular plates attached to spar hull. *Ships and Offshore Structures*, 2013: p. 1-17.
- [10] Sarpkaya, T. *Wave forces on offshore structures*. Cambridge University Press. 2010.